

**The potential energy surface and near-dissociation states of He- H 2 +**

Markus Meuwly and Jeremy M. Hutson

Citation: *The Journal of Chemical Physics* **110**, 3418 (1999); doi: 10.1063/1.478208

View online: <http://dx.doi.org/10.1063/1.478208>

View Table of Contents: <http://scitation.aip.org/content/aip/journal/jcp/110/7?ver=pdfcov>

Published by the [AIP Publishing](#)

---

**Articles you may be interested in**

[Full dimensional potential energy surface for the ground state of H 4 + system based on triatomic-in-molecules formalism](#)

*J. Chem. Phys.* **139**, 184302 (2013); 10.1063/1.4827640

[Time-dependent quantum wave packet study of the Ar+H<sub>2</sub> → ArH++H reaction on a new ab initio potential energy surface for the ground electronic state \(12 A'\)](#)

*J. Chem. Phys.* **138**, 174305 (2013); 10.1063/1.4803116

[Near-dissociation states and coupled potential curves for the HeN + complex](#)

*J. Chem. Phys.* **117**, 3109 (2002); 10.1063/1.1493176

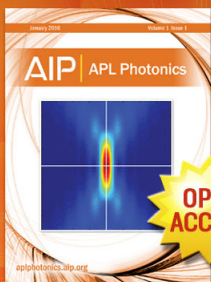
[Global potential energy surfaces for the H 3 + system. Analytical representation of the adiabatic ground-state 1 1 A' potential](#)

*J. Chem. Phys.* **112**, 1240 (2000); 10.1063/1.480539

[The potential energy surface and rovibrational states of He-HCO +](#)

*J. Chem. Phys.* **110**, 4347 (1999); 10.1063/1.478316

---



Launching in 2016!

The future of applied photonics research is here

**OPEN  
ACCESS**

**AIP** | APL  
Photonics

# The potential energy surface and near-dissociation states of He-H<sub>2</sub><sup>+</sup>

Markus Meuwly and Jeremy M. Hutson<sup>a)</sup>

*Department of Chemistry, University of Durham, South Road, Durham DH1 3LE, United Kingdom*

(Received 6 May 1998; accepted 28 October 1998)

The potential energy surface for the ground state of He-H<sub>2</sub><sup>+</sup> is calculated using *ab initio* QCISD(T) calculations and a correlation-consistent basis set. The geometries chosen include all combinations of 21 intermolecular distances  $R$ , three H-H distances  $r$ , and seven Jacobi angles  $\theta$ . The final potential is fitted to a functional form that incorporates the correct long-range behavior. Close-coupling calculations of both low-lying and near-dissociation vibration-rotation states are carried out. The results are expected to be of assistance in assigning the microwave spectra of He-H<sub>2</sub><sup>+</sup> in near-dissociation states [Carrington *et al.*, *Chem. Phys. Lett.* **260**, 395 (1996)]. © 1999 American Institute of Physics. [S0021-9606(99)01505-6]

## I. INTRODUCTION

Interactions between ionic species are of fundamental importance in physics and chemistry. However, much less is known about the potential energy surfaces that govern ionic interactions than about those for neutral species. Over the past few years, spectroscopic techniques have been developed to study ionic complexes, and these methods are very sensitive to details of the interaction potentials. The existence of the spectroscopic results provides a stimulus for developing accurate potential energy surfaces.

One very important prototype system is He-H<sub>2</sub><sup>+</sup>, for which Carrington's group in Southampton have recently observed a few microwave lines.<sup>1</sup> However, the experiment is an unusual one, and the lines are difficult to assign. In the Southampton experiment, a mass-selected ion beam containing highly excited He-H<sub>2</sub><sup>+</sup> molecules is subjected to microwave radiation, and then passed through an electric field. If the radiation populates states within a few cm<sup>-1</sup> of dissociation, they may be field-dissociated, and fragment H<sub>2</sub><sup>+</sup> ions are detected. However, since only microwave frequencies are involved, the initial state must also be very highly excited. The experiment thus selects ions that lie very close to dissociation.

The lines observed show no obvious pattern, but some of them show structure that must be due to nuclear hyperfine effects. Since He-H<sub>2</sub><sup>+</sup> can be formed from either para-H<sub>2</sub><sup>+</sup>, with total nuclear spin  $i=0$ , or as ortho-H<sub>2</sub><sup>+</sup>, with  $i=1$ , the structured lines must arise from ortho H<sub>2</sub>. However, the experiment by itself does not contain enough information to arrive at an assignment. In Ref. 1, bound-state calculations were carried out on a two-dimensional He-H<sub>2</sub><sup>+</sup> potential surface, and it was shown that vibration-rotation levels suitable to explain the spectra do exist near dissociation. However, the potential energy surface used<sup>2</sup> was not adequate to assign the spectra: in particular, it neglected any dependence on the H<sub>2</sub><sup>+</sup> bond length and truncated the angular expansion of the potential at  $P_2(\cos \theta)$ . The purpose of the present work is to describe a new and more complete potential energy surface,

obtained from high-level *ab initio* calculations, and to use it to investigate the near-dissociation levels of He-H<sub>2</sub><sup>+</sup> in more detail.

## II. THEORETICAL APPROACH

The quality of an *ab initio* potential energy surface (PES) depends greatly on the computational method and basis set used. In the present work, we have used the QCISD(T) method,<sup>3</sup> which is a variant of coupled-cluster theory that is equivalent to full (CI) for two-electron systems, and is size-consistent but not strictly variational. All calculations were carried out with the GAUSSIAN 94 program suite.<sup>4</sup> The main basis set used here is Dunning's aug-cc-pVQZ correlation-consistent basis set.<sup>5,6</sup> For He-H<sub>2</sub><sup>+</sup>, the aug-cc-pVQZ basis set consists of 145 uncontracted Gaussian-type orbitals (GTOs) including higher angular momentum and diffuse wavefunctions. There are 48 GTOs on each H atom ( $7s4p3d2f$  contracted to  $5s4p3d2f$ ) and 49 on the He atom ( $7s4p3d2f$  contracted to  $5s4p3d2f$ ).

The near-dissociation states involved in the microwave spectra of He-H<sub>2</sub><sup>+</sup> are particularly sensitive to the long-range part of the potential, so it is essential to describe the leading terms in the long-range expansion as accurately as possible. The most important long-range terms are the charge +induced dipole and quadrupole+induced dipole induction energies and the dispersion energy. The H<sub>2</sub><sup>+</sup> quadrupole moment  $\Theta(r)$  at  $r=1.9975 a_0$  calculated with the aug-cc-pVQZ basis set is  $1.5275 ea_0^2$ , which may be compared with an accurate value of  $1.531 ea_0^2$ ,<sup>7</sup> while the dipole polarizability  $\alpha_d$  for He calculated with this basis set is  $1.384 a_0^3$  compared to  $1.383 a_0^3$ .<sup>8</sup> The monomer properties are thus well reproduced by the basis set, and the long-range terms in the potential should be well represented.

The present work uses a standard Jacobi coordinate system, in which  $r$  is the H-H distance,  $R$  is the distance from the H-H midpoint to He, and  $\theta$  is the angle measured at the H-H midpoint. The grid on which energies were calculated was chosen to facilitate close-coupling calculations of the bound states. Evaluation of the necessary integrals is stablest if Gauss-Legendre points are used for the angular coordinate

<sup>a)</sup>Electronic mail: J.M.Hutson@durham.ac.uk

$\theta$ . We therefore performed calculations at angles corresponding to an 11-point quadrature ( $\theta=90^\circ, 74.36^\circ, 58.73^\circ, 42.1^\circ, 27.49^\circ, 11.98^\circ$ ; the remaining points are defined by symmetry). In addition, calculations were carried out for the linear configuration, which is where the global potential minimum lies. The H-H bond lengths chosen were  $r = 1.72 a_0, 2.00 a_0$  and  $2.37 a_0$ ;  $r = 2.00 a_0$  is very close to the free-monomer potential minimum at  $r = 1.997 23 a_0$ , and the other two points are the inner and outer turning points for the  $v=0$  state of the free monomer. The choice of  $r = 2.00 a_0$  for the central point facilitates comparison with previous work. The grid of intermolecular distances  $R$  included 21 points between  $2.1 a_0$  and  $14 a_0$ .

The intermolecular potential  $V(R, r, \theta)$  is defined as the electronic energy  $W(R, r, \theta)$  of the complex (supermolecule) with respect to that of the separated monomers *at the same  $H_2^+$  bond length*. In practice, it is important to include the counterpoise correction,<sup>9</sup> so that the monomer energies are calculated in the complete supermolecule basis set

$$\begin{aligned} V(R, r, \theta) &\approx V^{\text{corr}}(R, r, \theta) \\ &= W_{\text{HeH}_2^+}(R, r, \theta) - W_{\text{He}}(R, r, \theta) - W_{\text{H}_2^+}(R, r, \theta). \end{aligned} \quad (1)$$

Comparison of these monomer energies with those calculated in the monomer basis sets alone shows that the counterpoise correction is no larger than  $5 \text{ cm}^{-1}$  in the region of the potential well.

The full potential energy surface that describes the  $\text{HeH}_2^+$  complex is

$$E(R, r, \theta) = V(R, r, \theta) + V_{\text{H}_2^+}(r), \quad (2)$$

where  $V_{\text{H}_2^+}(r)$  is the potential curve for isolated  $\text{H}_2^+$ , chosen here to be zero at its minimum. The distinction between  $V(R, r, \theta)$  and  $E(R, r, \theta)$  is crucial when discussing ‘‘equilibrium’’ properties: the well depths and equilibrium geometries referred to in this section are those of  $E(R, r, \theta)$ . The ‘‘well depths’’ quoted here are thus energies with respect to the separated monomers with  $\text{H}_2^+$  at its equilibrium geometry.

There are always approximations involved in the construction of an *ab initio* PES. The quality of the actual surface can be assessed if calculations are performed at other correlation levels and with different basis sets. The complete surface was therefore recalculated using the smaller aug-cc-pVDZ and aug-cc-pVTZ (with 33 and 76 uncontracted GTOs, respectively). The comparison of the counterpoise-corrected energies may be summarized as follows:

- (1) The aug-cc-pVDZ basis gives a potential that is shallower by about  $2 mE_h$  ( $400 \text{ cm}^{-1}$ ) than those obtained with the larger bases. The equilibrium distance  $R_e$  is also larger.
- (2) The aug-cc-pVTZ and aug-cc-pVQZ basis sets give results fairly similar to one another, with a difference of about  $150 \mu E_h$  ( $30 \text{ cm}^{-1}$ ) between the well depths and  $0.002 a_0$  between the  $R_e$  values.
- (3) In the very long-range part of the interaction, all three basis sets predict very similar interaction energies.

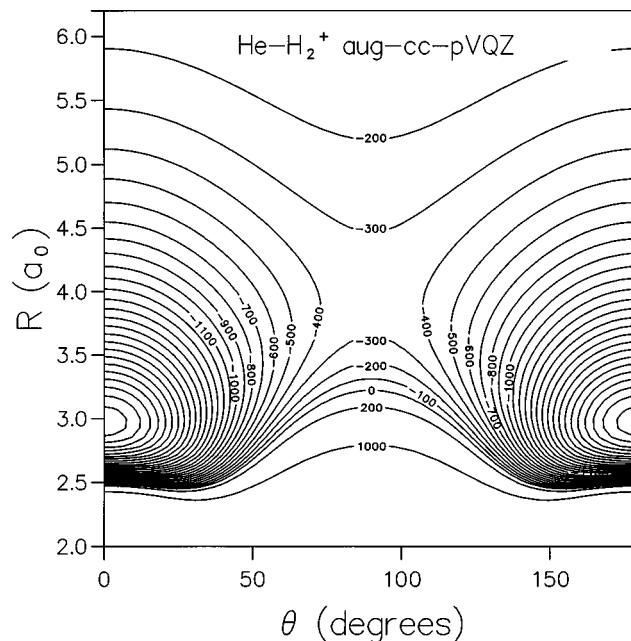


FIG. 1. Contour plot of the QCISD(T) aug-cc-pVQZ potential for  $\text{He-H}_2^+$  with  $r$  fixed at  $2.0 a_0$ . Contours are shown (in  $\text{cm}^{-1}$ ) relative to  $\text{H}_2^+(r=2.0 a_0) + \text{He}$  at  $R = \infty$ .

Increasing the size of the basis sets shows the expected convergence of the *ab initio* energies. Fitting the energies to an exponentially decaying function as a function of the basis size leads to predictions for arbitrarily large basis sets (so-called complete basis set extrapolation CBSE<sup>10</sup>). The extrapolation gives a well depth about  $7 \mu E_h$  ( $1.5 \text{ cm}^{-1}$ ) deeper than the aug-cc-pVQZ basis set, with equilibrium values  $R_e$  and  $r_e$  changed by less than  $10^{-3} a_0$ . These changes may be taken as a reasonable estimate of the basis-set incompleteness errors in the aug-cc-pVQZ results.

In view of the importance of the long-range energy for  $\text{He-H}_2^+$ , it is crucial to check the sensitivity of the energies to the addition of extra diffuse functions. We therefore carried out test calculations with supplementary diffuse *s*, *p*, *d* and *f* functions, and obtained virtually unaltered interaction energies over the whole range of  $R$ .

To test the adequacy of the QCISD(T) correlation treatment, a one-dimensional cut was calculated for the collinear configuration at  $r = 2.00 a_0$  using coupled-cluster theory at the CCSD(T) level. The energies deviate by no more than  $0.5 \text{ cm}^{-1}$  from the QCISD(T) results over the whole range of the intermolecular distance  $R$ .

A two-dimensional cut through the three-dimensional PES for  $r = 2.00 a_0$  is shown in Fig. 1. The deep linear minimum with a steep repulsive wall is characteristic of protonated complexes. In the T-shaped configuration, the attraction is much weaker and the repulsive wall is less steep.

Selected features of the present aug-cc-pVQZ potential are compared with previous potentials in Table I. The two-dimensional surface of Falcetta and Siska<sup>2</sup> (F/S) was calculated for  $r = 2.0 a_0$  only, using MCSCF MRCI calculations with a  $5s3p1d$  basis set for H and a  $6s3p1d$  basis set for He. Their surface may be compared with the corresponding cut through the aug-cc-pVQZ potential. The present potential is

TABLE I. Comparison of features of different He-H<sub>2</sub><sup>+</sup> potential energy surfaces.

|                           | M/T               | S/K   | This work | F/S             | This work |
|---------------------------|-------------------|-------|-----------|-----------------|-----------|
|                           | Three-dimensional |       |           | Two-dimensional |           |
| $D_e$ (cm <sup>-1</sup> ) | 2560              | 2646  | 2717      | 2504            | 2669      |
| $D_0$ (cm <sup>-1</sup> ) | 1793              | 1710  | 1754      | 1484            | 1593      |
| $R_e$ ( $a_0$ )           | 2.977             | 2.976 | 2.972     | 2.978           | 2.970     |
| $r_e$ ( $a_0$ )           | 2.074             | 2.073 | 2.075     | 2.00            | 2.00      |

about 150 cm<sup>-1</sup> deeper, and has a value of  $R_e$  (for  $r = 2.0 a_0$ ) that is about 0.008  $a_0$  smaller. However, the two potentials are very similar at long range. The differences at short range principally reflect the larger basis set used in the present work.

Our potential may also be compared with earlier three-dimensional surfaces. The absolute well depth of our potential is 2717 cm<sup>-1</sup>, which is substantially greater than that obtained by McLaughlin and Thompson<sup>11,12</sup> (M/T, 2560 cm<sup>-1</sup>) but much closer to that for the potential of Špirko and Kraemer<sup>13</sup> (S/K, 2646 cm<sup>-1</sup>). M/T performed SCF-CI calculations based on a double zeta (DZP) basis set, which is much smaller than the one used here. In the more recent work by Špirko and Kraemer, the basis set was 9s4p3d for He and 8s4p3d for H, contracted to 4s3p2d in each case. This is still somewhat smaller than ours. S/K included correlation at the MRCI level, with molecular orbitals previously optimized in a CASSCF calculation.

The comparisons above show that our potential has most of the same qualitative features as those reported but should be more accurate. In addition, it includes sufficient points at long range to make it appropriate for use in studying the near-dissociation states.

### III. FITTING THE *AB INITIO* POINTS

Dynamical calculations usually require an analytic form for the interaction potential. Before describing the form that we used, it is useful to consider how much can be extracted without least-squares fitting.

It is convenient to expand the potential in terms of radial strength functions  $V(R, r)$  and Legendre polynomials  $P_\lambda(\cos \theta)$

$$V(R, r, \theta) = \sum_{\lambda} V_{\lambda}(R, r) P_{\lambda}(\cos \theta). \quad (3)$$

Only terms with  $\lambda$  even occur because H<sub>2</sub><sup>+</sup> is homonuclear. Since the calculations were done at Gauss-Legendre quadrature points, it is straightforward to project out the radial strength functions for  $\lambda \leq 10$ . The results of this are shown for  $r = 2.00 a_0$  in Fig. 2. It may be seen that there are appreciable attractive wells in all the radial strength functions up to  $\lambda = 6$ , and even  $\lambda = 8$  has a well about 0.8 cm<sup>-1</sup> deep.

In the present work, the *ab initio* energies are fitted to an  $r$ -dependent functional form based on the fixed- $r$  form used by Falcetta and Siska.<sup>2</sup> This provides a reasonable compromise between accuracy and simplicity for present purposes,

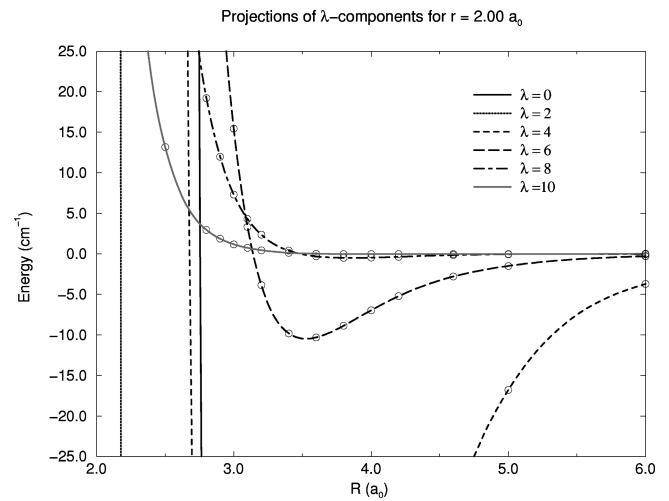


FIG. 2. Legendre components of the QCISD(T) aug-cc-pVQZ potential for He-H<sub>2</sub><sup>+</sup> with  $r$  fixed at  $2.0 a_0$ .

though it introduces some problems at large  $r$  and small  $R$ , and we intend to develop a more satisfactory global function in future work.

The radial strength functions are split into a short-range and a long-range contribution

$$V_{\lambda}(R, r) = V_{\lambda}^{\text{short}}(R, r) + V_{\lambda}^{\text{long}}(R, r). \quad (4)$$

The short-range part is written (for  $\lambda \leq 6$ ) as a Morse-like potential

$$V_{\lambda}^{\text{short}}(R, r) = A_{\lambda}(r) \exp[-\beta_{\lambda}(r)R] - B_{\lambda}(r) \exp[-\frac{1}{2}\beta_{\lambda}(r)R]. \quad (5)$$

The attractive part for  $\lambda \leq 6$  is needed to take account of the wells in the radial distribution functions described above. For  $\lambda = 8$ , the attractive term is omitted and a purely repulsive form is used instead

$$V_{\lambda}^{\text{short}}(R, r) = A_{\lambda}(r) \exp[-\beta_{\lambda}(R - R_{m,00})], \quad (6)$$

where  $R_{m,00}$  is the constant term in the quadratic expansion of  $R_{m,\lambda}(r) = \sum_{k=0}^2 R_{m,\lambda,k}(r - r_m)^k$  (see below). The term with  $\lambda = 10$  was found to make very little difference to the quality of the fit, and was not included.

The long-range part of the functional form is chosen to take account of the terms up to  $R^{-6}$  in the interaction between a neutral S-state atom with dipole and quadrupole polarizabilities  $\alpha_d$  and  $\alpha_q$  and a homonuclear  $\Sigma$ -state molecular ion with charge  $q$  and quadrupole moment  $\Theta(r)$

$$V_0^{\text{long}}(R, r) = -\frac{\alpha_d q^2}{2R^4} - \frac{\alpha_q q^2}{2R^6} - \frac{C_6^{(0)}(r)}{R^6}, \quad (7)$$

$$V_2^{\text{long}}(R, r) = -\frac{3q\alpha_d\Theta(r)}{R^6} - \frac{C_6^{(2)}(r)}{R^6}, \quad (8)$$

$$V_{\lambda}^{\text{long}}(R, r) = 0 \quad \text{for } \lambda > 2. \quad (9)$$

Each term proportional to  $R^{-n}$  in the long-range expansion is damped by multiplying it by a Tang-Toennies damping function<sup>14</sup>

TABLE II. Parameters for He-H<sub>2</sub><sup>+</sup> M/H potential, fitted to the QCISD(T)/aug-cc-pVQZ potential energy surface. Energies are expressed in  $mE_h$  and lengths in  $a_0$ .

| Parameter       | Value      | 95% Confidence limit | Parameter       | Value      | 95% Confidence limit |
|-----------------|------------|----------------------|-----------------|------------|----------------------|
| $\epsilon_{00}$ | 3.322157   | 0.015                | $\epsilon_{40}$ | 1.002369   | 0.038                |
| $\epsilon_{01}$ | -1.807461  | 0.038                | $\epsilon_{41}$ | 1.979361   | 0.097                |
| $\epsilon_{02}$ | 2.0248948  | 0.174                | $\epsilon_{42}$ | 1.91426    | 0.423                |
| $\beta_{00}$    | 2.1751111  | 0.017                | $\beta_{40}$    | 3.4954174  | 0.057                |
| $\beta_{01}$    | -0.2861302 | 0.043                | $R_{m,40}$      | 3.07792542 | 0.010                |
| $\beta_{02}$    | 0.527239   | 0.187                | $R_{m,41}$      | 0.0798258  | 0.018                |
| $R_{m,00}$      | 3.42049171 | 0.005                | $\epsilon_{60}$ | 0.075046   | 0.024                |
| $R_{m,01}$      | 0.4213555  | 0.011                | $\epsilon_{61}$ | 0.2006160  | 0.072                |
| $R_{m,02}$      | -0.466017  | 0.052                | $\beta_{60}$    | 3.3311841  | 0.257                |
| $\epsilon_{20}$ | 11.130449  | 0.056                | $R_{m,60}$      | 3.4612064  | 0.056                |
| $\epsilon_{21}$ | 9.784067   | 0.102                | $R_{m,61}$      | 0.4269003  | 0.108                |
| $\epsilon_{22}$ | 2.34964    | 0.456                | $A_8$           | 0.00497486 | 0.004                |
| $\beta_{20}$    | 3.174869   | 0.023                | $\beta_8$       | 5.515032   | 0.838                |
| $\beta_{21}$    | 0.21225    | 0.078                |                 |            |                      |
| $R_{m,20}$      | 2.62814797 | 0.005                |                 |            |                      |
| $R_{m,21}$      | 0.0705369  | 0.015                |                 |            |                      |

$$D_{n,\lambda}(R,r) = 1 - \exp[-\beta_\lambda(r)R] \sum_{k=0}^n \frac{[\beta_\lambda(r)R]^k}{k!}. \quad (10)$$

The long-range expansion used here does not contain explicit terms of order  $R^{-8}$  and higher; any such terms are incorporated into the attractive coefficients  $B_\lambda(r)$  in the short-range potential.

The H<sub>2</sub><sup>+</sup> quadrupole moment  $\Theta(r)$  and the isotropic and anisotropic components of the He-H<sub>2</sub><sup>+</sup> dispersion coefficient  $C_6(r)$  have recently been fitted to analytical expressions.<sup>15</sup> These expressions were used unchanged in the present fit. In particular, it may be noted that the dispersion coefficients  $C_6(r)$  increase quadratically for large values of  $r$ , and do not reach a constant limiting value as  $r \rightarrow \infty$ .

In the actual fit, the quantities varied for  $\lambda \leq 6$  are the well depth  $\epsilon_\lambda(r)$  and the position of the radial minimum  $R_{m,\lambda}(r)$  rather than  $A_\lambda(r)$  and  $B_\lambda(r)$ . There is a simple unique correspondence between these two sets of parameters as described in Eqs. (41) to (45) in Ref. 16.

Parameterizing in terms of  $\epsilon_\lambda(r)$  and  $R_{m,\lambda}(r)$  has conceptual advantages: they are easier to visualize than  $A_\lambda(r)$  and  $B_\lambda(r)$ , and preliminary estimates to initiate the fit can be made by inspection of the projections  $V_\lambda(R,r)$  of the *ab initio* energies.

In the present work,  $r$  dependence was introduced by expanding the parameters  $\epsilon_\lambda(r)$ ,  $R_{m,\lambda}(r)$  (or  $A_\lambda(r)$  for  $\lambda = 8$ ) and  $\beta_\lambda(r)$  as quadratic polynomials about the monomer equilibrium separation (taken to be  $r_m = 2.00 a_0$ ): thus  $\beta_\lambda(r) = \sum_{k=0}^2 \beta_{\lambda,k}(r - r_m)^k$  and so forth. This gives a total of 38 parameters that can be varied.

The most important region of the potential for spectroscopic purposes is the negative-energy region. Accordingly, we carried out weighted least-squares fits, with all negative-energy points weighted equally (uncertainty  $\pm 10 \mu E_h$ ) but positive-energy points given less weight (uncertainty  $\pm \max(10^{-3} V, 10 \mu E_h)$ ).

The fitting was performed using I-NoLLS,<sup>17</sup> which is an interactive fitting package that allows the user to adjust pa-

rameters selectively and apply physical insight to guide the progress of a least-squares fit. Parameters that are poorly determined, and do not add usefully to the flexibility of the function, can be identified and eliminated as the fit progresses. The final set of 29 fitted parameters is given in Table II. The deviations between the fitted potential values and the *ab initio* points are primarily concentrated on the repulsive wall. The largest absolute error in the bound-state region is less than  $50 \mu E_h$  ( $10 \text{ cm}^{-1}$ ), and most of the points are fitted within  $5 \mu E_h$  ( $1 \text{ cm}^{-1}$ ). On the repulsive wall, the deficiencies of the functional form and the larger deviation of the *ab initio* points allowed in the fit lead to larger errors. Examples of these effects are shown in Fig. 3.

#### IV. BOUND-STATE CALCULATIONS

A major aim of the present work is to assist in assigning the microwave spectra involving near-dissociation states of He-H<sub>2</sub><sup>+</sup>.<sup>1</sup> There are several sources of angular momentum in the complex, and an account of the angular momentum coupling scheme needed to describe the states has been given previously.<sup>1</sup> Following the usual convention for van der Waals complexes, lower-case letters are used for all monomer quantum numbers to distinguish them from those for the complex as a whole. In the H<sub>2</sub><sup>+</sup> monomer, the electron spin  $s$  and the total nuclear spin  $i$  first couple to form a resultant  $g$ . The rotational angular momentum of the nuclei about one another is designated  $r$ , and couples with  $g$  to form the total angular momentum  $f$ . The fine and hyperfine splittings due to this coupling are less than 100 MHz, so are several orders of magnitude smaller than the separations between rotational levels. Two separate sets of ro-vibrational levels exist, one corresponding to para-H<sub>2</sub><sup>+</sup> ( $i=0$ ) and one corresponding to ortho-H<sub>2</sub><sup>+</sup> ( $i=1$ ). Only levels with even  $r$  are allowed for  $i=0$  and only levels with odd  $r$  are allowed for  $i=1$ .

In the He-H<sub>2</sub><sup>+</sup> complex, the effect of the potential anisotropy is to mix the H<sub>2</sub><sup>+</sup> rotational levels, so that  $r$  is no longer a good quantum number (though the mixing is small enough

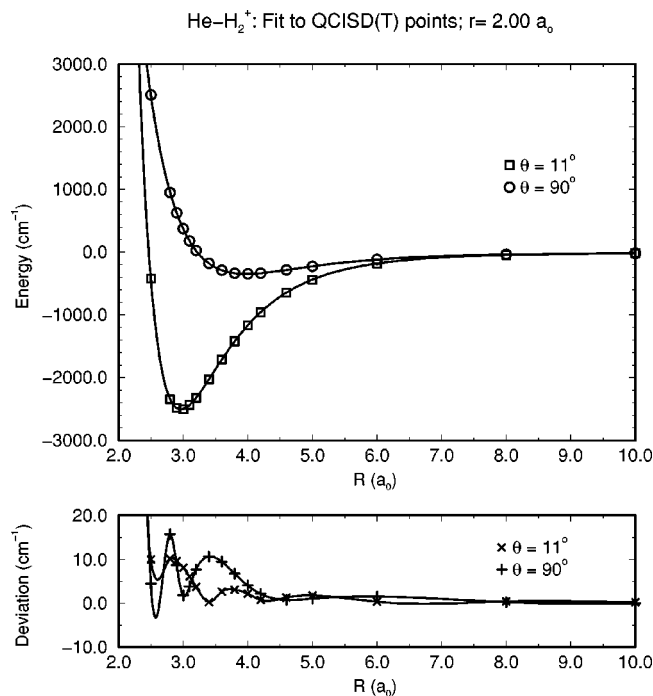


FIG. 3. Quality of the fit to the *ab initio* points for  $\text{He-H}_2^+$ . The upper panel shows the potential itself for  $r=2.0 a_0$  and two different angles, and the lower panel shows the differences between the calculated points and the fitted function.

near dissociation that  $r$  is still a useful label there). The projection of  $r$  onto the intermolecular axis is denoted  $\mathcal{R}$ , and is nearly conserved (apart from Coriolis matrix elements that couple states with  $\Delta\mathcal{R} = \pm 1$ ). The total mechanical angular momentum is denoted  $N$ , and also has body-fixed projection  $\mathcal{R}$ . In the complex,  $g$  is no longer coupled directly to  $r$ . Instead,  $g$  couples with  $N$  to form the total angular momentum  $F$ . However, since the fine and hyperfine terms that couple  $g$  to  $N$  are again very weak (less than 100 MHz),  $s$  and  $i$  can to a first approximation be neglected in calculating the vibration-rotation levels, and reintroduced when interpreting the fine and hyperfine structure. This is the approach taken in the present work.

The quantum numbers used here for the levels of  $\text{He-H}_2^+$  are thus  $r$ ,  $\mathcal{R}$  and  $N$ . Readers familiar with closed-shell complexes may note that these are analogous to the familiar  $j$ ,  $K$  and  $J$ , respectively. As for closed-shell species, levels with  $\mathcal{R}=0$  have  $e$  symmetry while those with  $|\mathcal{R}|>0$  are split by Coriolis coupling into pairs with  $e$  and  $f$  symmetry.

We have used the BOUND program<sup>18</sup> to carry out close-coupling calculations of the bound vibrational-rotation states supported by the fitted potential in both two and three dimensions. The total wavefunction is expanded using a basis set of  $\text{H}_2^+$  rotational or vibrotational functions for the four angular coordinates and the H-H distance  $r$ , and the resulting coupled equations in  $R$  are solved numerically using a log-derivative propagator.<sup>19</sup> The methods used are described in detail in Ref. 20. The calculations are actually carried out in a space-fixed basis set, but this does not affect the resulting energies.

The  $\text{He-H}_2^+$  reduced mass is taken to be  $1.3403216 m_u$

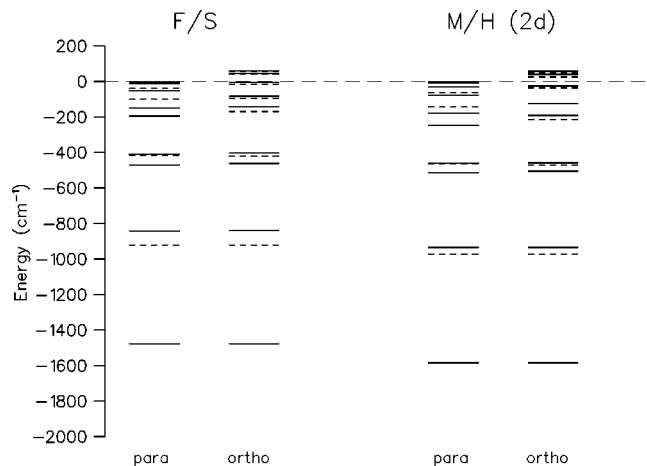


FIG. 4. Comparison between the calculated vibrational levels for the present potential (M/H) (with  $r$  constrained to  $2.0 a_0$ ) and the potential of Falcetta and Siska (F/S) (which was calculated for  $r=2.0 a_0$  only). The dashed lines represent levels with  $\mathcal{R}=1$ , which do not exist for  $N=0$ .

( $m_u = m_a(^{12}\text{C})/12$ ). The coupled equations are propagated from  $R_{\min}=1.6 a_0$  to  $R_{\max}=40 a_0$ , extrapolating to zero step size from log-derivative interval sizes of 0.05 and  $0.10 a_0$  using Richardson  $h^4$  extrapolation. Increasing the propagation range or decreasing the step size changes the eigenvalues by less than  $10^{-6} \text{ cm}^{-1}$ .

## A. Results on the two-dimensional potentials

The bound states of the present PES can be compared with those obtained previously for the two-dimensional potential of Falcetta and Siska (F/S). For this comparison, the  $\text{H}_2^+$  monomer separation is fixed at  $r=2.00 a_0$ . This gives an  $\text{H}_2^+$  rotor constant  $b=29.866 \text{ cm}^{-1}$ . The basis set used includes all angular channels correlating with  $\text{H}_2^+$  rotor levels up to  $r=13$ . Separate calculations are carried out for para- $\text{H}_2^+$  (even  $r$ ) and ortho- $\text{H}_2^+$  (odd  $r$ ), since even and odd levels are not mixed by the intermolecular potential.

The two-dimensional calculations on the present surface give a ground-state binding energy of  $1593 \text{ cm}^{-1}$ , compared to  $1484 \text{ cm}^{-1}$  for the F/S potential. The patterns of vibrational states are compared in Fig. 4, and it may be seen that the two potentials give qualitatively similar results. The differences are due principally to the different well depths of the two potentials: even for near-dissociation levels, the absolute level positions depend on the amount of phase space in the well region.

The near-dissociation states just below the ortho- $\text{H}_2^+$  and para- $\text{H}_2^+$  dissociation thresholds are of particular interest, since these are the states which might be detected in the Southampton experiment.<sup>1</sup> The near-dissociation levels on the two potentials are compared in Fig. 5; they are reasonably similar, but it may be seen that the new potential gives some parity splittings that are inverted compared to those on the F/S potential. This is a subtle effect arising from the differences in the well depths for the linear and T-shaped geometries for the two potentials, but serves to emphasize the importance of using a high-quality potential.

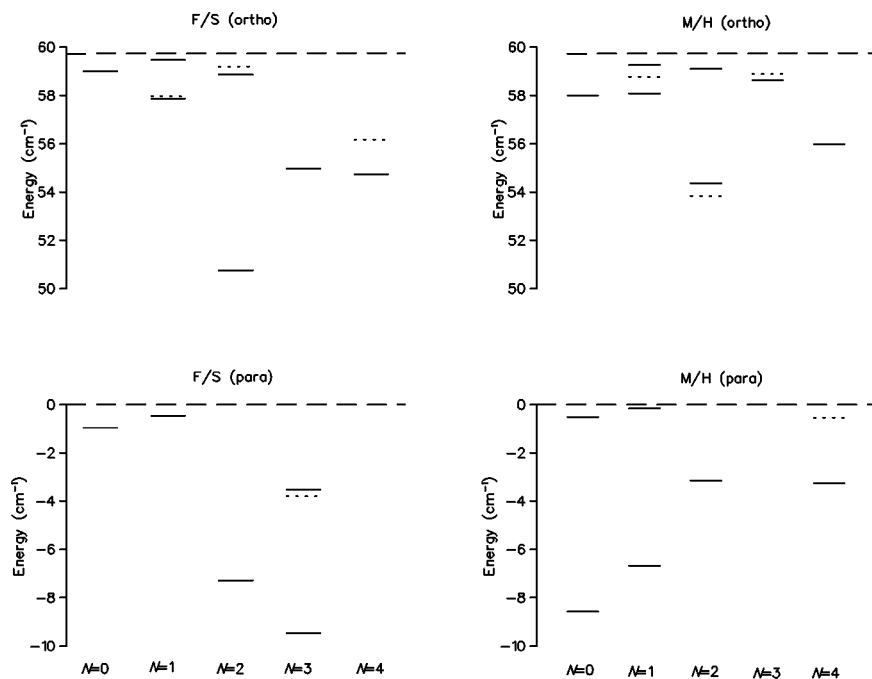


FIG. 5. Comparison between the calculated near-dissociation states for the present potential (M/H) (with  $r$  constrained to  $2.0 a_0$ ) and the potential of Falchetta and Siska (F/S) (which was calculated for  $r=2.0 a_0$  only). States of  $e$  symmetry are shown as solid lines, and states of  $f$  symmetry as dotted lines.

## B. Results on the three-dimensional potentials

Calculations on a two-dimensional potential are a useful first approximation, but for complexes with large binding energies such as  $\text{He-H}_2^+$  the intermolecular potential is strong enough to cause significant mixing of the vibrational monomer states.<sup>21</sup> To take this into account, calculations on the full three-dimensional potential are needed, with explicit basis functions for the  $r$  coordinate.

Three-dimensional close-coupling calculations require an accurate and efficient means of evaluating matrix elements between monomer vibrational functions. In the present work, we use the quadrature scheme proposed by Schwenke and Truhlar.<sup>22</sup> We chose to use a three-point quadrature based on the three  $\text{H}_2^+$  bond lengths for which the *ab initio* calculations were performed. Anharmonic  $\text{H}_2^+$  vibrational wavefunctions are calculated using the LEVEL program<sup>23</sup> and an  $\text{H}_2^+$  potential energy function calculated with the aug-cc-pVQZ basis set at the Hartree-Fock level: no correlation is needed because  $\text{H}_2^+$  is a one-electron system. Separate weights are determined for each vibrational matrix element ( $v, v'$  pair). The weights are chosen so that integrals over potential terms constant, linear and quadratic in  $r$  are evaluated exactly. The one-dimensional potential is virtually identical to the one reported by Bishop and Wetmore.<sup>24</sup>

The basis sets used for the three-dimensional calculations include all channels correlating with  $\text{H}_2^+$  vibration-rotation states ( $v, r$ ) with  $r+2v \leq 13$ . Test calculations showed that the eigenvalues are converged to within  $10^{-2} \text{ cm}^{-1}$  with respect to the basis size.

The bound-state calculations require monomer vibration-rotation energies as input. To provide these, the one-dimensional Schrödinger equation was solved using LEVEL and the  $\text{H}_2^+$  potential described above. The results for some levels of  $\text{He-H}_2^+$  are remarkably sensitive to the eigenvalues used. We investigated the differences introduced by supplying instead the eigenvalues from recent calculations on  $\text{H}_2^+$

including relativistic and radiative corrections.<sup>25</sup> The effect is an overall shift of all energy levels downwards by about  $0.6 \text{ cm}^{-1}$  in the region of the potential well and by smaller amounts for states near dissociation. The frequencies of transitions involving near-dissociation states shift by up to 13 GHz. In the remainder of this work the vibration-rotation energies calculated with the  $\text{H}_2^+$  aug-cc-pVQZ potential are used.

The vibrational levels supported by the present three-dimensional *ab initio* PES are compared with those for the M/T and S/K potentials in Fig. 6. The binding energy for the ground vibration-rotation state of the complex on the present potential is  $1754 \text{ cm}^{-1}$ . This compares with  $1793 \text{ cm}^{-1}$  on the M/T potential<sup>26</sup> and  $1710 \text{ cm}^{-1}$  on the S/K<sup>13</sup> potential. The pattern of the lower-lying energy levels is similar to that for the S/K potential. However, the patterns near dissociation are very different: this arises because the present potential

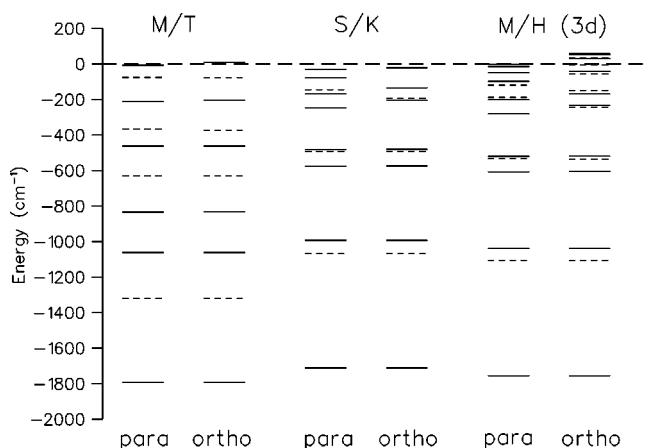


FIG. 6. Comparison between the calculated vibrational levels for the present potential (M/H) with  $r$  unconstrained and the potentials of McLaughlin and Thompson (M/T) and Špirko and Kraemer (S/K). The dashed lines represent levels with  $R=1$ , which do not exist for  $N=0$ .

TABLE III. Calculated band origins and spectroscopic parameters for the lowest few vibrational levels of He-H<sub>2</sub><sup>+</sup>.

| Vibrational level              | $E_v/hc$<br>(cm <sup>-1</sup> ) | $B_v/hc$<br>(cm <sup>-1</sup> ) | $D_v/hc$<br>(10 <sup>-4</sup> cm <sup>-1</sup> ) |
|--------------------------------|---------------------------------|---------------------------------|--|
| Ground state (ortho)           | -1754.269                       | 4.1193                          | 3.96   |
| Ground state (para)            | -1754.251                       | 4.1194                          | 3.96   |
| Bend ( <i>f</i> ) (ortho)      | -1107.989                       | 4.1089                          | 5.61   |
| Bend ( <i>f</i> ) (para)       | -1107.878                       | 4.1086                          | 5.59   |
| Bend ( <i>e</i> ) (ortho)      | -1108.163                       | 3.9367                          | 10.21  |
| Bend ( <i>e</i> ) (para)       | -1108.054                       | 3.9343                          | 9.96   |
| Intermolecular stretch (ortho) | -1038.379                       | 3.7171                          | 1.23   |
| Intermolecular stretch (para)  | -1038.412                       | 3.7190                          | 1.35   |

has the correct inverse power form near dissociation, whereas the S/K potential was fitted using exponential functions. The results for the older M/T potential show a substantially different pattern of energy levels, even for the low-lying states, and a totally different pattern near dissociation.

The existing experiments<sup>1</sup> probe the high-lying states of He-H<sub>2</sub><sup>+</sup>. However, other experiments may certainly be envisaged. We have calculated the vibration-rotation energy levels for  $N=0$  to 5 for the lowest few vibrational states of He-H<sub>2</sub><sup>+</sup>, and have fitted the resulting energy levels to a conventional expansion for a linear molecule

$$E_v(N, \mathcal{R}) = E_v + B_v [N(N+1) - \mathcal{R}^2] - D_v [N(N+1) - \mathcal{R}^2]^2. \quad (11)$$

The resulting spectroscopic constants are shown in Table III. It is possible that millimeter-wave transitions corresponding to pure rotational transitions could be observed either in the laboratory or in interstellar gas clouds, where He-H<sub>2</sub><sup>+</sup> may well exist. In addition, infrared spectra may be observable: two of the three fundamental vibrations are calculated with band origins at 716 cm<sup>-1</sup> (intermolecular stretch) and 646 cm<sup>-1</sup> (bend). As expected, the rotational constants change only slightly with bending excitation, but decrease quite substantially with stretching excitation. The low-lying states are very similar for ortho-He-H<sub>2</sub><sup>+</sup> and para-He-H<sub>2</sub><sup>+</sup>, since the corresponding wavefunctions are essentially localized in the two equivalent linear wells: the ortho and para states correspond to odd and even combinations of the localized states, and are separated by a tunneling splitting which is only 0.01792 cm<sup>-1</sup> for the vibrational ground state.

It is interesting to compare the frequencies in Table III (from fully anharmonic bound-state calculations) with the harmonic frequencies of 986, 721 and 1937 cm<sup>-1</sup>, calculated from the second derivatives of the potential at the minimum. It may be seen that the harmonic bending and stretching frequencies are both substantially too high. The excited H-H stretching state actually lies above dissociation, and is substantially broadened by predissociation. Bound-state calculations with an artificial wall placed in the potential at  $R = 25 a_0$  show that this state actually lies approximately 1825 cm<sup>-1</sup> above the ground state.

Calculations of the near-dissociation states were performed for angular momentum up to  $N=6$ . The levels lying between the  $r=0$  and  $r=1$  dissociation limits, calculated on the two- and three-dimensional potentials, are displayed in

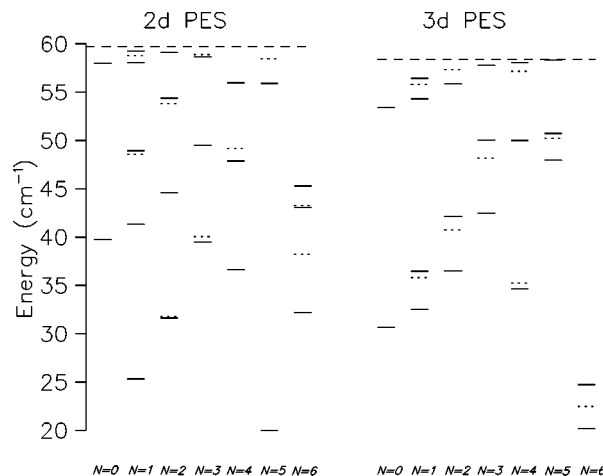
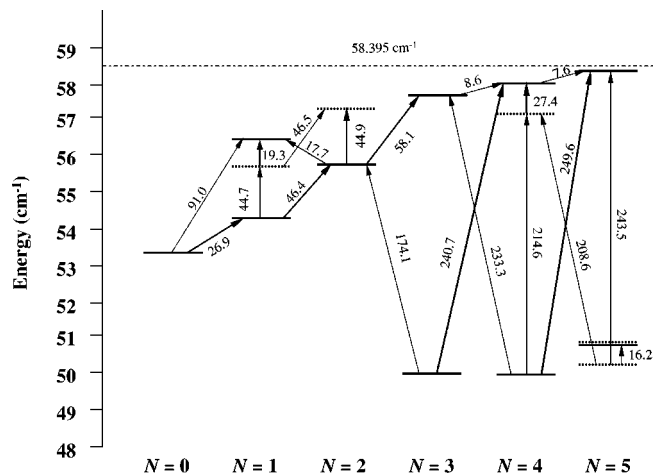


FIG. 7. Comparison between the high-lying ortho states for the two-dimensional and three-dimensional versions of the present potential.

Fig. 7. This shows the different  $\mathcal{R}$ -stacks running as singlets or doublets from low to high  $N$  values (recall that  $\mathcal{R}$  represents the projection of  $r$  onto the intermolecular axis). The level pattern shows clear differences from the one obtained from calculations on the two-dimensional potential. A more detailed view of the level pattern is shown in Fig. 8, which focuses on states that might be accessible to the microwave experiment. For all total  $N$  values considered, the three-dimensional calculations show one or more extra levels near the  $r=1$  dissociation limit.

There are some bound states near dissociation for  $N > 6$ , but we have found no pairs of levels with  $\Delta N = 0$  or  $\pm 1$  that might give rise to observable microwave transitions.

Parity doublets are of particular interest because the best studied of the experimental microwave transitions (near 15.2 GHz) is a complicated multiplet that seems likely to originate from an  $e-f$  transition across an  $\mathcal{R}$ -doublet in ortho-He-H<sub>2</sub><sup>+</sup>.<sup>1</sup> Two  $|\mathcal{R}|=1$  progressions provide possible candidates for this transition. The first exists for  $N=1$  and 2, but is above the dissociation threshold for  $N \geq 3$  even on the new

FIG. 8. Calculated near-dissociation states and predicted transition frequencies (in GHz) for ortho-He-H<sub>2</sub><sup>+</sup>. States of *e* symmetry are shown as solid lines, and states of *f* symmetry as dotted lines. Pure rotational transitions are indicated with thicker lines.

potential. However, a second progression exists for  $N=1, 2, 3$  and  $4$ , and the  $N=4$  doublet is close enough to dissociation for the transition to be observable. It is interesting (and surprising) to note that the splitting is nowhere near proportional to  $(N+1/2)$  as would be expected from simple arguments: indeed, the calculated splitting for  $N=4$  is actually smaller than that for  $N=3$ . The probable explanation of this is that the observed splitting arises from a competition between two different Coriolis interactions, with  $\mathcal{R}=0$  states lying both above and below the  $|\mathcal{R}|=1$  levels, and the relative positions of the perturbing levels change quite fast with  $N$ .

The  $N=4$  levels for  $|\mathcal{R}|=1$  do not exist in the two-dimensional calculations. However, the corresponding  $N=3$  levels exist in both calculations, and it may be seen that they are bound by about  $7\text{ cm}^{-1}$  more in the three-dimensional case.

Intensity considerations lead to the conclusion that the  $15.2\text{ GHz}$  transition probably has  $N>2$ .<sup>27</sup> The  $N=4$  parity doublet is thus an attractive candidate. The calculated frequency is  $27.4\text{ GHz}$ , but it is quite sensitive to details of the calculation, because of the competition between Coriolis interactions described above. It is thus plausible that reasonably small changes in the potential could bring it into agreement with experiment.

In order to assess the sensitivity of the calculated frequencies to the quality of the analytical fit, we have also carried out calculations on a potential that interpolates between the *ab initio* points, using the reproducing kernel Hilbert space (RKHS) method.<sup>28</sup> The calculated eigenvalues near dissociation differ by up to  $0.4\text{ cm}^{-1}$  and the transition frequencies by comparable amounts. As an example, the  $27.4\text{ GHz}$  splitting of the  $N=4$  parity doublet calculated on the fitted PES increases to  $31.3\text{ GHz}$  if calculated on the interpolated potential.

Another parity doublet sequence runs from  $N=5$  down to  $N=1$ , though none of its levels are close enough to dissociation to be promising candidates for the  $15.2\text{ GHz}$  transition. Between  $N=4$  and  $N=3$  the ordering in the  $e$  and  $f$  states changes. This is again due to competition between Coriolis interactions with nearby  $\mathcal{R}=0$  states.

The bound-state calculations provide wavefunctions that are useful in understanding the near-dissociation states. The wavefunctions from the full close-coupling calculations are difficult to visualize, because they are nonseparable functions of four angles as well as the two distances  $R$  and  $r$ . However, helicity decoupling calculations, which preserve the projection quantum number  $\mathcal{R}$ , can also be performed, and these provide wavefunctions that can be factorized to give functions of the body-fixed angle  $\theta$ . Contour plots of a few such wavefunctions for ortho states are shown in Fig. 9. Apart from the ground state, which is included for comparison, all the states shown lie within  $6\text{ cm}^{-1}$  of dissociation. It may be seen that the near-dissociation states have wavefunctions that peak at  $R=10$  to  $12 a_0$ . They have fairly pure  $r=1$  character at long range ( $R>6 a_0$ ), but the nodal structure is considerably more complicated at shorter range, where basis functions with  $r\geq 3$  are important.

Expectation values of quantities such as  $R$  and  $P_2(\cos\theta)$  are more compact than complete wavefunctions, and can help to understand them. Values for these expectation values are given in Table IV. We find that  $\langle R \rangle$  is larger than  $8 a_0$  for all calculated near-dissociation states. The expectation value  $\langle P_2(\cos\theta) \rangle$  would be  $+0.4$  for a pure  $r=1, \mathcal{R}=0$  state and  $-0.2$  for a pure  $r=1, |\mathcal{R}|=1$  state. The values in Table IV show that even the  $f$  component of the  $N=4, |\mathcal{R}|=1$  doublet is significantly mixed; the deviation from  $-0.2$  in this case is a measure of the extent of mixing of  $r=3$  character.

An apparently isolated pair of very closely spaced levels appears for  $N=5$  about  $10\text{ cm}^{-1}$  below dissociation. Inspection of angular and radial expectation values shows that these are in fact an  $|\mathcal{R}|=2$  doublet, with a very small parity splitting. These states have  $\langle R \rangle \approx 3.6 a_0$ , whereas the  $|\mathcal{R}|=1$  states just above them have  $\langle R \rangle \approx 8 a_0$ .

Figure 8 shows the calculated frequencies of some of the allowed transitions that might be observable experimentally. Most of the transitions seen so far are observed by detecting ionic fragments arising from electric field dissociation of the complex, and this can take place only if one of the levels involved is within a few  $\text{cm}^{-1}$  of dissociation. The dipole moment operator has odd parity, so that the selection rules are  $e \leftrightarrow f$  for  $\Delta N=0$  and  $e \leftrightarrow e$  and  $f \leftrightarrow f$  for  $\Delta N = \pm 1$ .

## V. CONCLUSIONS

We have carried out high-level *ab initio* calculations of the potential energy surface for  $\text{He-H}_2^+$  at the QCISD(T) level, using a very large basis set (aug-cc-pVQZ). We have fitted the resulting points to a three-dimensional functional form that incorporates the correct long-range behavior, and have used the fitted potential to carry out close-coupling calculations of bound states all the way from the potential minimum to dissociation.

Our fitted potential is the best available for calculating the near-dissociation states of  $\text{He-H}_2^+$  involved in the spectra of Carrington *et al.*<sup>1</sup> Earlier potentials either neglected the H-H stretching coordinate or used fitting functions without the correct long-range behavior. The new potential has more bound states near dissociation than the two-dimensional potential of Falcetta and Siska, which was used in earlier attempts to assign the near-dissociation spectra. Our results suggest that the experimentally observed<sup>1</sup> multiplet near  $15.2\text{ GHz}$  is probably between a pair of near-dissociation levels with quantum numbers  $r=1, N=4$  and  $|\mathcal{R}|=1$ .

The remaining discrepancy between the experimental and calculated frequencies may have several sources. Limitations in the basis set and the correlation treatment used in the *ab initio* calculations probably lead to a small underestimate of the interaction energy. This may produce an overall shift of the energy levels, but is unlikely to alter the energy-differences between nearby states enough to bring experiment and theory into agreement. However, changes in the  $\text{H}_2^+$  threshold energies input to the bound-state calculation can affect the near-dissociation frequencies by several GHz. In addition, the errors due to fitting the potential may be significant: when the potential points are interpolated instead

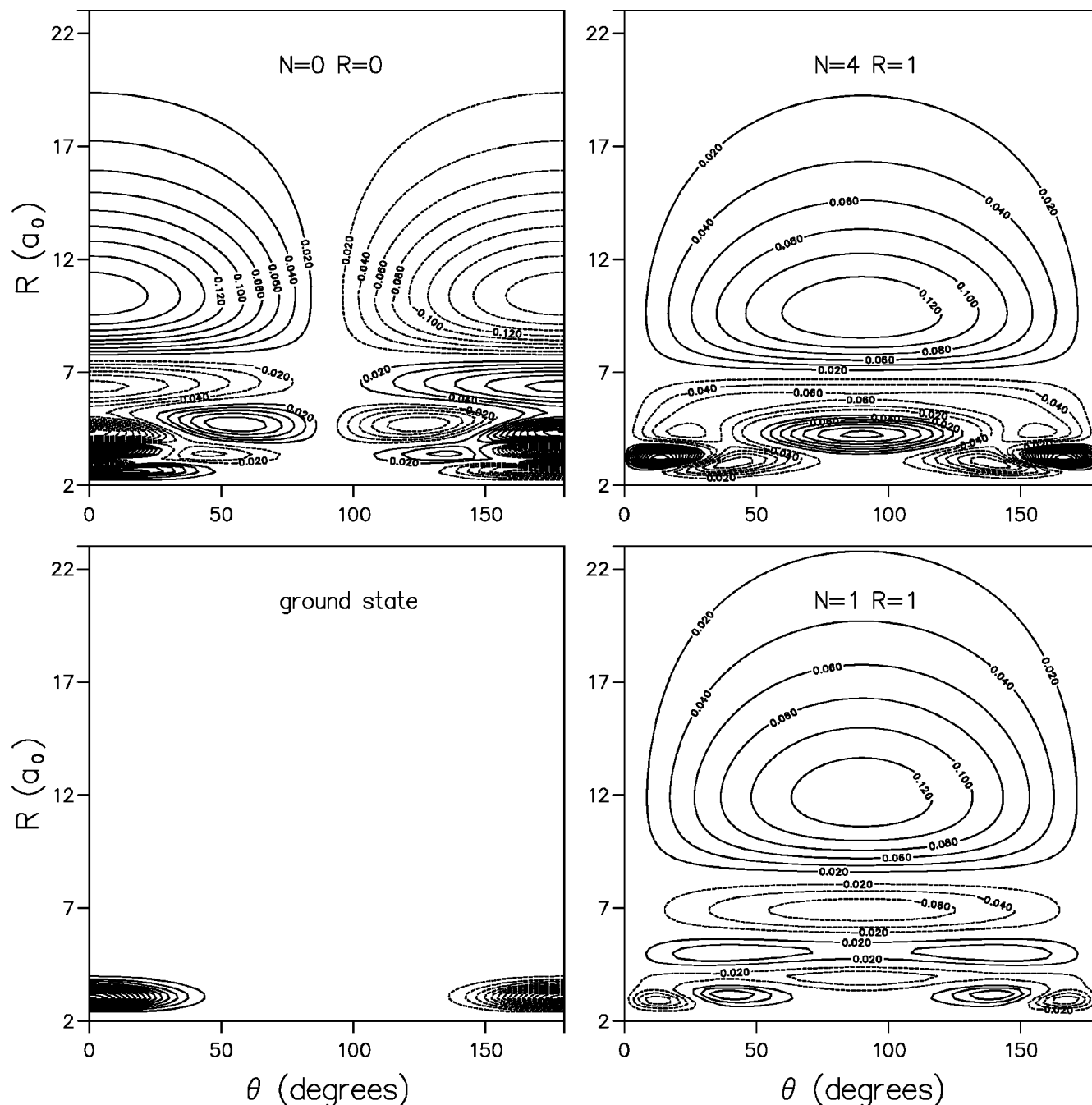


FIG. 9. Calculated wave functions from helicity decoupling calculations on states of ortho  $\text{He-H}_2^+$ . In addition to the ground state, the levels shown lie near  $53 \text{ cm}^{-1}$  ( $N=0, R=0$ ),  $56 \text{ cm}^{-1}$  ( $N=1, R=1$ ) and  $58 \text{ cm}^{-1}$  ( $N=4, R=1$ ).

of fitted, the transition frequency of the  $N=4$  parity doublet changes by about 4 GHz. Such effects might be responsible for the remaining disagreement. Alternatively, the discrepancy could be due to breakdown of the Born-Oppenheimer approximation. It is known that the adiabatic and nonadiabatic corrections to dissociation energies are of the order of  $20 \text{ cm}^{-1}$  for  $\text{H}_2^+$ <sup>29</sup> and  $2 \text{ cm}^{-1}$  for  $\text{H}_3^+$ .<sup>30</sup> Analogous effects may be expected for  $\text{He-H}_2^+$ , and may have a significant effect on the near-dissociation states.

The functional form used in the present work provides a good fit in the region of the potential well, but is not entirely satisfactory on the repulsive wall and may not be accurate enough for high-energy inelastic scattering calculations. In

TABLE IV. Energies and expectation values for near-dissociation states of  $\text{He-H}_2^+$ .

| $(N, R)$ | Parity   | $E/hc \text{ (cm}^{-1}\text{)}$ | $\langle R \rangle \text{ (a}_0\text{)}$ | $\langle P_2(\cos \theta) \rangle$ |
|----------|----------|---------------------------------|--|------------------------------------|
| 0,0      | <i>e</i> | 53.4061                         | 9.59                                     | 0.3589                             |
| 1,1      | <i>f</i> | 55.7954                         | 12.71                                    | -0.1868                            |
| 1,0      | <i>e</i> | 54.3041                         | 11.01                                    | 0.2008                             |
| 1,1      | <i>e</i> | 56.4396                         | 12.74                                    | -0.0116                            |
| 2,1      | <i>f</i> | 57.3461                         | 14.30                                    | -0.1896                            |
| 2,0      | <i>e</i> | 55.8489                         | 12.52                                    | 0.1290                             |
| 3,0      | <i>e</i> | 57.7841                         | 15.64                                    | 0.1227                             |
| 4,1      | <i>f</i> | 57.1585                         | 9.61                                     | -0.1427                            |
| 4,1      | <i>e</i> | 58.0708                         | 12.09                                    | -0.0524                            |
| 5,0      | <i>e</i> | 58.3247                         | 9.97                                     | 0.2622                             |

addition, it does not include the  $\text{HeH}^+ + \text{H}$  reactive channel. The development of a global functional form which is adequate for these purposes will be the subject of future work.

## ACKNOWLEDGMENTS

M. M. acknowledges financial support from the Schweizerischer Nationalfonds zur Förderung der wissenschaftlichen Forschung. The calculations were carried out on a Silicon Graphics Origin 2000 computer system, which was purchased with funding from the Engineering and Physical Sciences Research Council. We are grateful to Dr. Lydia Heck for computational assistance.

- <sup>1</sup>A. Carrington, D. I. Gammie, A. M. Shaw, S. M. Taylor, and J. M. Hutson, *Chem. Phys. Lett.* **260**, 395 (1996).
- <sup>2</sup>M. F. Falcetta and P. E. Siska, *Mol. Phys.* **88**, 647 (1996).
- <sup>3</sup>J. A. Pople, M. Head-Gordon, and K. Raghavachari, *J. Chem. Phys.* **87**, 5968 (1987).
- <sup>4</sup>M. J. Frisch, G. W. Trucks, H. B. Schlegel, P. M. W. Gill, B. G. Johnson, M. A. Robb, J. R. Cheeseman, T. Keith, G. A. Petersson, J. A. Montgomery, K. Raghavachari, M. A. Al-Laham, V. G. Zakrzewski, J. V. Ortiz, J. B. Foresman, J. Cioslowski, B. B. Stefanov, A. Nanayakkara, M. Challacombe, C. Y. Peng, P. Y. Ayala, W. Chen, M. W. Wong, J. L. Andres, E. S. Replogle, R. Gomperts, R. L. Martin, D. J. Fox, J. S. Binkley, D. J. Defrees, J. Baker, J. P. Stewart, M. Head-Gordon, C. Gonzalez, and J. A. Pople, *GAUSSIAN 94*, revision E.2, 1995.
- <sup>5</sup>T. H. Dunning, Jr., *J. Chem. Phys.* **90**, 1007 (1989).
- <sup>6</sup>R. A. Kendall, T. H. Dunning, Jr., and R. J. Harrison, *J. Chem. Phys.* **96**, 6796 (1992).

- <sup>7</sup>D. M. Bishop and B. Lam, *Mol. Phys.* **65**, 679 (1988).
- <sup>8</sup>D. M. Bishop and J. Pipin, *Chem. Phys. Lett.* **236**, 15 (1995).
- <sup>9</sup>S. F. Boys and F. Bernardi, *Mol. Phys.* **19**, 553 (1970).
- <sup>10</sup>D. E. Woon and T. H. Dunning, Jr., *J. Chem. Phys.* **99**, 1914 (1993).
- <sup>11</sup>D. R. McLaughlin and D. L. Thompson, *J. Chem. Phys.* **70**, 2748 (1979).
- <sup>12</sup>T. Joseph and N. Sathyamurthy, *J. Chem. Phys.* **86**, 704 (1987).
- <sup>13</sup>V. Špirko and W. P. Kraemer, *J. Mol. Spectrosc.* **172**, 265 (1995).
- <sup>14</sup>K. T. Tang and J. P. Toennies, *J. Chem. Phys.* **80**, 3726 (1984).
- <sup>15</sup>J. M. Hutson and A. Ernesti, *Mol. Phys.* (accepted).
- <sup>16</sup>A. Carrington, C. A. Leach, A. J. Marr, A. M. Shaw, M. R. Viant, J. M. Hutson, and M. M. Law, *J. Chem. Phys.* **102**, 2379 (1995).
- <sup>17</sup>M. M. Law and J. M. Hutson, *Comput. Phys. Commun.* **102**, 252 (1997).
- <sup>18</sup>J. M. Hutson, BOUND computer program, version 5, distributed by Collaborative Computational Project No. 6 of the UK Engineering and Physical Sciences Research Council, 1993.
- <sup>19</sup>B. R. Johnson, *J. Comput. Phys.* **13**, 445 (1973).
- <sup>20</sup>J. M. Hutson, *Comput. Phys. Commun.* **84**, 1 (1994).
- <sup>21</sup>M. Meuwly and R. J. Bemish, *J. Chem. Phys.* **106**, 8672 (1997).
- <sup>22</sup>D. W. Schwenke and D. G. Truhlar, *Comput. Phys. Commun.* **34**, 57 (1984).
- <sup>23</sup>R. J. Le Roy, LEVEL computer program, University of Waterloo Chemical Physics Report No. CP 330, 1992.
- <sup>24</sup>D. M. Bishop and R. W. Wetmore, *Mol. Phys.* **26**, 145 (1973).
- <sup>25</sup>R. E. Moss, *Mol. Phys.* **80**, 1541 (1993).
- <sup>26</sup>J. Tennyson and S. Miller, *J. Chem. Phys.* **87**, 6648 (1987).
- <sup>27</sup>A. Carrington (private communication).
- <sup>28</sup>T. S. Ho and H. Rabitz, *J. Chem. Phys.* **104**, 2584 (1996).
- <sup>29</sup>G. Hunter and H. O. Pritchard, *J. Chem. Phys.* **46**, 2153 (1967).
- <sup>30</sup>B. M. Dinelli, C. R. Le Sueur, J. Tennyson, and R. D. Amos, *Chem. Phys. Lett.* **232**, 295 (1995).